Analysis of Permanent Magnet Demagnetization during the Starting Process of a Line-start Permanent Magnet Synchronous Motor

Tuan Le Anh
Hanoi University of Industry, Vietnam
tuanla1@haui.edu.vn

Thuy Trinh Bien
Vietnam–Korea College of Quang Ninh, Vietnam
trinhthuyvhqn@gmail.com

Cuong Ngo Xuan
School of Engineering and Technology, Hue University, Vietnam
ngoxuancuong@hueuni.edu.vn

Tuan Do Anh
Dai Nam University, Vietnam
doanhtuan@dainam.edu.vn

Y. Do Nhu
Hanoi University of Mining and Geology, Vietnam
donhuy@humg.edu.vn (corresponding author)

Received: 31 July 2024 | Revised: 19 August 2024, 12 September 2024, and 20 September 2024 | Accepted: 22 September 2024

 DOI: https://doi.org/10.48084/etasr.8576

ABSTRACT

Neodymium (NdFeB) rare earth Permanent Magnets (PMs) are widely used in the manufacturing of Line-Start Permanent Magnet Synchronous Motors (LSPMSMs). During the initial startup of LSPMSMs, irreversible PM demagnetization often occurs. This research provides a thorough examination of the PM demagnetization process during the initiation of a 15-kW, 3000-rpm LSPMSM, which was converted from a squirrel-cage Induction Motor (IM) featuring a 3-bar PM. Utilizing Ansys/Maxwell2D software for simulations and conducting experiments, this study reveals that upon starting the LSPMSM, demagnetization occurs at the two outermost PM pairs. This leads to unstable motor operation at synchronous speed, significant current fluctuations, and a substantial decrease in performance. The findings suggest that to ensure effective LSPMSM operation, it is crucial to either restrict frequent restarts or select an appropriate PM type to prevent partially irreversible demagnetization, thereby enhancing power efficiency.

Keywords-neodymium; LSPMSM; partial irreversible demagnetization; starting current

I. INTRODUCTION

Currently, Neodymium (NdFeB) rare-earth Permanent Magnets (PM) are widely used in the manufacturing of high-performance motors, including Line-Start Permanent Magnet Synchronous Motors (LSPMSMs) [1, 2]. LSPMSMs have the advantages of high efficiency and a large Power Factor (PF) and have gradually proven to be an alternative to squirrel-cage Induction Motors (IMs) [2-4]. However, it is essential to calculate the PM design to avoid irreversible demagnetization in an LSPMSM motor [5]. The phenomenon of partial irreversible demagnetization of the PM adversely affects the working parameters and performance of the LSPMSM, and these parameters may even be lower than those of the IM [6, 7].

The phenomenon of PM demagnetization in an LSPMSM can occur for many different reasons, one of which is during the starting process of the LSPMSM. A simulation study of a 3.7 kW and 2-pole LSPMSM with a rotor structure and three PM bars showed that when starting, an increased starting current of up to 80 A can cause partial demagnetization of the PM [6]. To avoid this phenomenon, the angle of the PM arrangement was changed to reduce the starting current, thereby avoiding the partial demagnetization of the PM [6]. However, this study did not demonstrate the influence of demagnetization on the working characteristics of an LSPMSM. In [7], partial irreversible demagnetization of 15 kW and 4-pole LSPMSM was presented, but this research only stopped at studying the points where demagnetization can occur with "W-type" PM structure and with a 1500 rpm motor. Demagnetization of the LSPMSM can occur when starting [8, 9], as well as due to coil short circuits in the stator winding [10], and abnormal conditions [11]. In [12], the effect of rotor resistance on demagnetization in the case of continuous starting was analyzed, and to avoid demagnetization, it was necessary to reduce the rotor resistance of the LSPMSM, therefore reducing motor heating and synchronization time.

Numerous studies have documented the demagnetization phenomenon in LSPMSMs during start-up. Certain studies have identified that the starting current, temperature increase during startup, and PM layout influence partial PM demagnetization. However, the impact of partial demagnetization on the working parameters of a 3000-rpm LSPMSM converted from an IM during startup or the demagnetization potential of PM pairs has not been studied. This research aims to thoroughly evaluate and analyze the demagnetization phenomenon in a 3000-rpm LSPMSM converted from an IM with a 3-bar PM structure. Using the Finite Element Method (FEM) via Ansys/Maxwell2D software, the demagnetization of LSPMSM was simulated and the working parameters during startup as well as the demagnetization level of the PM pairs were investigated. Additionally, the simulation results were verified through an experimental LSPMSM model.

II. LSPMSM AND DEMAGNETIZATION

LSPMSM is essentially a combination of a PM Synchronous Motor (PMSM) and an IM by placing PM bars in the rotor of IM (Figure 1) [2, 13]. A 3000-rpm LSPMSM was converted from IM with a 3-bar PM rotor structure arranged as shown in Figure 1. To ensure good working parameters for the LSPMSM, it is necessary to avoid PM demagnetization during motor operation [5, 6].

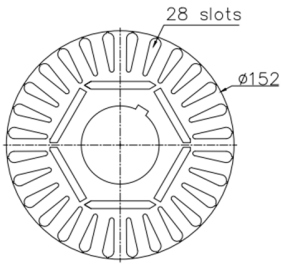

Fig. 1. 3000-rpm LSPMSM rotor configuration.

The demagnetization is usually expressed in two forms, $B(H)$ and $J(H)$, and the working point of the PM during the operation of the LSPMSM on the demagnetization characteristic is the intersection of the load characteristic line with straight line $B(H)$, as evidenced in Figure 2 [14].

When power is supplied to the stator coil of the LSPMSM, the magnetic flux density of the PM is determined by [15]:

$$B_m = B_r + \mu_r \mu_0 . H_m \quad (1)$$

where B_m is the magnetic flux density in T, B_r is the residual induction in T, H_m is the demagnetizing field in A/m, μ_0 is the vacuum magnetic permeability in N/A^2, and μ_r is the magnetic permeability.

From Figure 2, it can be observed that when designing a motor in the rated mode, the working point (point a) demagnetization characteristic ($B_m.\mu_0 H_m$) is often chosen such that the residual energy in the PM, i.e. [$B_m. \mu_0.H_m$] is maximum [5].

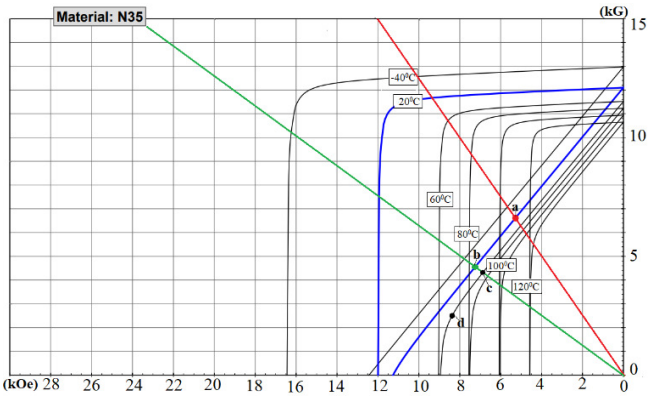

Fig. 2. Demagnetization characteristic curve of NdFeB-N35 PM.

When LSPMSM starts, the starting current will increase about 4-8 times the rated current. Then the load characteristic of the motor will change from load line to load line 1, the working point on the demagnetization characteristic will change to workpoint-1 (point b) point [$B_{m1}. \mu_0.H_{m1}$].

In some cases, such as continuous starting, the temperature of the motor at the start time increases (greater than 20 ^oC). Assuming the motor starts at a temperature of 60 ^oC, the working point on the demagnetization characteristic is workpoint-2 (point c) and on the demagnetization characteristic, an irreversible demagnetization point called the "knee" point will appear (Figure 2). When the working point workpoint-2 exceeds the "knee" (point d) point counterclockwise, irreversible partial demagnetization occurs. The phenomenon of partial demagnetization of the PM affects the working parameters of an LSPMSM.

III. PM DEMAGNETIZATION DURING LSPMSM START-UP

The demagnetization level of the magnet bar pairs is not the same; therefore, it is important to investigate and evaluate the

demagnetization level of the components, hence investigate the working characteristics of the LSPMSM.

A. Evaluation of LSPMSM Start-up Demagnetization Capability

The motor parameters of the LSPMSM were a speed of 3000 rpm, power of 15 kW, working voltage of 380/660 V, and frequency of 50 Hz. The LSPMSM was converted from an IM type 160M [2, 16]. The PM arranged in the LSPMSM was type N35 with three bars, and the size of each bar was b.h = 35.8 (mm.mm), as depicted in Figure 1.

The FEM approach was deployed through the Ansys/Maxwell2D software to study the electromagnetic field distribution and working characteristics of the LSPMSM [17]. The research results for the working characteristics of the LSPMSM are shown in Figure 3.

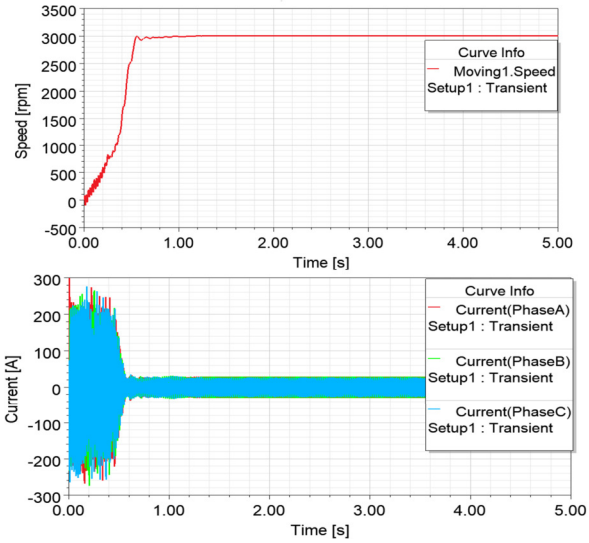

Fig. 3. Working characteristics of the LSPMSM: (a) speed and (b) current.

The results in Figure 3 demonstrate that the proposed LSPMSM can completely start and synchronize after a period t=0.58 s, the working current was approximately 26.4 A, while the maximum starting current of the motor reached 162 A. However, the starting pulse currents reached 278 A, which was high enough to induce irreversible partial demagnetization of the PM. Figure 4 portrays the simulation results of the magnetic flux density distribution 150 ms after the start-up. According to Figure 4, the PM had the highest magnetic field attenuation at its corner positions, corresponding to points N1–N6, as shown in Figure 5. Points N1 and N6 are the points that are most likely to be demagnetized. The results of the magnetic flux density analysis at point N1 over time during the start-up process are displayed in Figure 6.

The results in Figure 6 exhibit that under the effect of the external magnetic field generated by the starting current during the starting process, the magnetic inductance at point N1 changes over time and has the smallest value B_{min} = 0.061 T at time t_{min} = 235 ms. Similar surveys for points N2 to N6 provide the results listed in Table I.

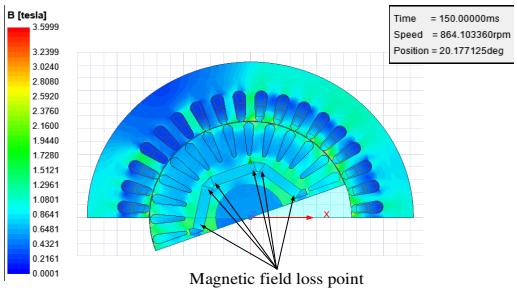

Fig. 4. Magnetic flux density distribution at 150 ms.

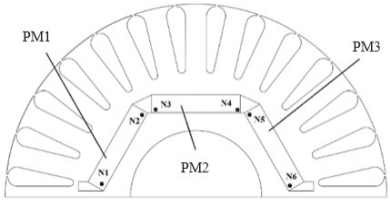

Fig. 5. Survey point of working magnetic flux density of the PM.

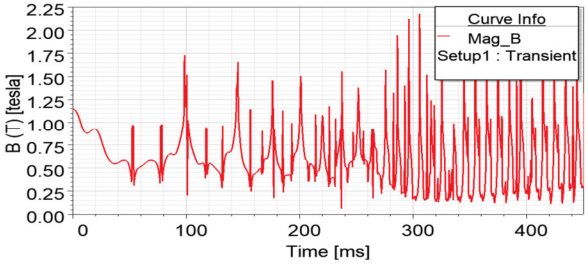

Fig. 6. Magnetic flux density distribution of point N1 on PM1 over time.

TABLE I. B_{MIN} VALUE OF EACH SELECTED POINT

Point	PM1		PM2		PM3	
	N1	N2	N3	N4	N5	N6
B_{min} (T)	0.061	0.028	0.1	0.086	0.025	0.078
t_{min} (ms)	235	135	300	405	498	278

The results in Table I demonstrate that with the above 3-bar PM structure, the two outer PM bars have the working points with the smallest magnetic field, that is, point N5 (B_{minN5} = 0.025 T) at 498 ms and N2 (B_{minN2} = 0.028 T) at 135 ms. This proves that among the three PM bars, the two outer magnet bars are easier to demagnetize during the starting process.

When the starting motor temperature is 60 °C, the magnetic field at the knee point is B_{knee} = 0.3 T (Figure 2), which leads to PM demagnetization from the minimum point N5 (B_{minN5} = 0.025 T) to the maximum point N3 (B_{minN3} = 0.1 T). If the motor starts in the temperature range of 20 °C to 60 °C, there is the easiest possibility of irreversible demagnetization at point N5 (B_{minN5} = 0.025 T). Thus, under the starting condition of the motor, irreversible partial demagnetization may occur for one or two pairs of PMs in the outermost part of the LSPMSM.

B. Effect of Demagnetization Phenomenon on the Working Characteristics of LSPMSM

The LSPMSM start-up demagnetization evaluation results revealed that point N5 on the PM3 pair had the smallest residual magnetism (B_{minN5} = 0.025 T), followed by point N2 on

the PM1 pair (B_{minN2} = 0.028 T), which is likely to be demagnetized next. To analyze the effect of demagnetization on the working characteristics of the LSPMSM, a research scenario was proposed by assuming that PM3 (point N5) has a 30% loss of magnetic field (70% remaining magnetic field), and PM1 has a 35% loss of magnetic field (65% remaining magnetic field) owing to the demagnetization phenomenon during the starting process.

The results of the starting and current characteristics of the LSPMSM when the two pairs of PM3 and PM1 were partially demagnetized are shown in Figure 7.

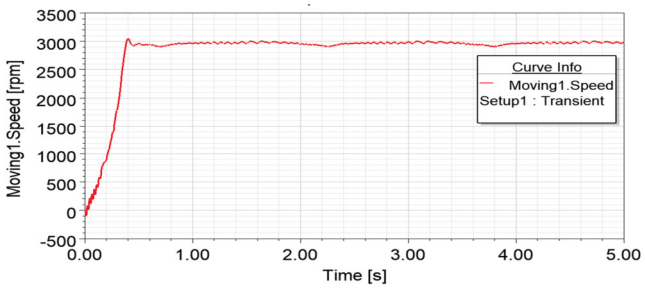

Fig. 7. Speed characteristics of partially demagnetized motor.

According to the results in Figure 7, the time for LSPMSM to start and reach synchronous speed is about 0.4 s, which is shorter than the time of 0.58 s noted in Figure 1. This can be explained by the fact that the magnetism of PM1 and PM2 was reduced; thus, the static magnetic attraction of the rotor and stator was reduced, making the starting time faster. However, owing to the partial demagnetization phenomenon, the LSPMSM cannot operate stably at synchronous speed. Therefore, it operates below synchronous speed, and the motor speed fluctuates with strong oscillation amplitude, causing vibration and noise during operation.

The current graph in Figure 8 shows that after the starting time (0.4 s), the working current of the motor is unstable, the current amplitude fluctuates significantly, and the current increases (the maximum effective value was 50.3 A), which is about 1.9 times higher compared to the case of no demagnetization of 26.4 A (Figure 3b). The high current causes an increase in the temperature, which can lead to PM demagnetization under the normal working conditions of the LSPMSM.

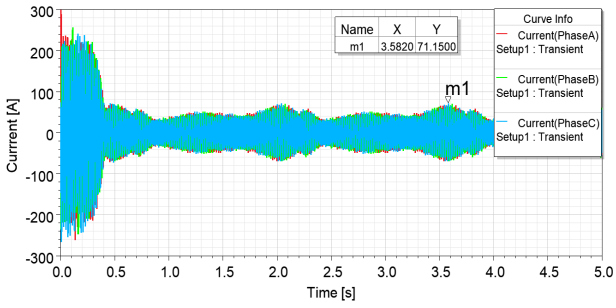

Fig. 8. Current characteristics of partially demagnetized motor.

In addition, the LSPMSM efficiency is determined by the electromagnetic and mechanical power characteristics, as illustrated in Figure 9. The corresponding simulation in the two modes demonstrated that the motor efficiency without demagnetization was 92.8%, and the motor efficiency with partial demagnetization without recovery (Figure 9) was 90.1%. The motor efficiency was significantly reduced by 2.7%, which was lower than that of the same type of IM (90.3%).

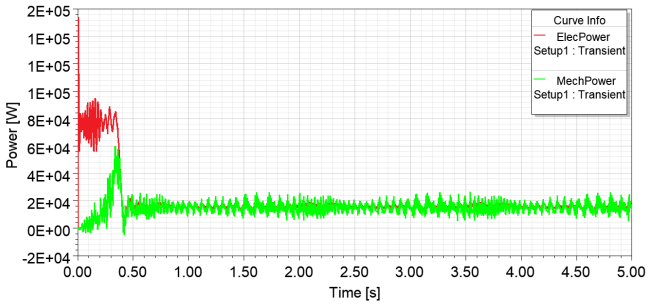

Fig. 9. Electromagnetic power and mechanical power of LSPMSM.

The results of the simulation model disclose that during the LSPMSM start-up process with a 3-bar structure, the two outer bars are most easily demagnetized, and the demagnetization level of the bars is not the same. In the case of two pairs of partially demagnetized magnets, the LSPMSM's working characteristics are much worse. For example, the working speed fluctuates, leading to a loss of synchronization, the current amplitude fluctuates greatly, and the motor efficiency is greatly reduced with the parameters analyzed.

IV. EXPERIMENTAL STUDY ON THE EFFECT OF DEMAGNETIZATION PHENOMENON

The purpose of this experiment was to determine the accuracy of the theoretical and simulation results. The studied LSPMSM was made from a rotor with a three-bar PM structure with the same parameters as those analyzed above. The experiment was conducted at the Hanoi Electromechanical Manufacturing Joint Stock Company (HEM), as depicted in Figure 10. Throughout the experiment, a generator load regulator (also known as the excitation regulator) was used to modify the motor load. A KYORITSU 6310 multifunction power analyzer was deployed to measure the electrical parameters. This measurement device is limited to recording the voltage, current, and PF data. Due to its extended sampling time, the results are calculated over a prolonged period, making the comparison with the simulation results approximate. Initially, the LSPMSM started and ran with a rated load for a sufficiently long time for the mechanical temperature to steadily increase. The test results of the current and PF characteristics in Figure 11 indicate that when the motor starts, the current value of the phases is approximately 26 A (Figure 11a), PF = 0.94 (Figure 11b), and the calculated efficiency is 92.57%, which is similar to the simulation results shown in Figures 3 and 9. By surveying the motor housing temperature with a Fluke-59 Max heat gun, it was found that the temperature of the motor housing reached 60 °C.

(a)

(b)

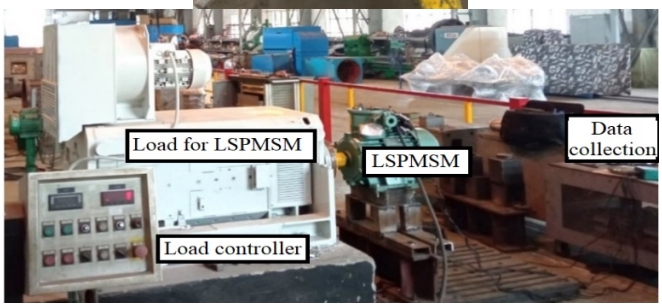

Fig. 10. Test model for performing the experiments. (a) Fabricated rotor and (b) complete system.

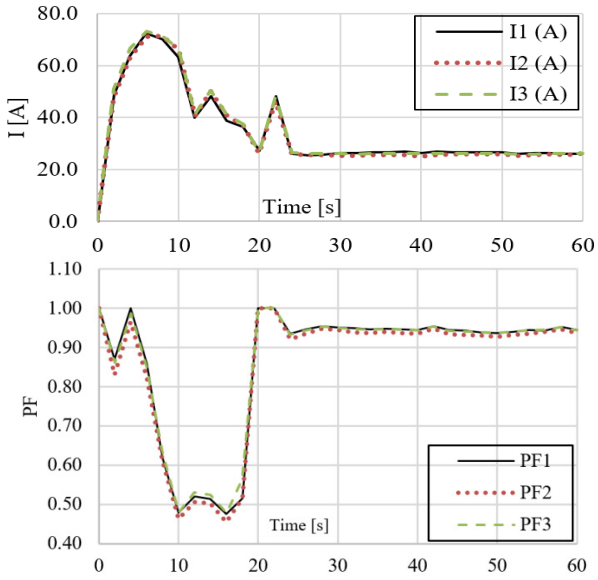

Fig. 11. Current and PF characteristics without demagnetization.

The experimental findings depicted in Figure 12 indicate that the motor current was not stable, fluctuating between 26.2 A and 31.2 A. The average current value reached 28.9 A, approximately 1.1 times higher than the initial value. Additionally, the PF decreased to PF = 0.9, while the efficiency was 87.19%. These results demonstrate that the LSPMSM operated unstably at synchronous speed. Consequently, the PM experienced partial non-recoverable demagnetization, which aligns with the simulation outcomes presented in Figures 7 and 8.

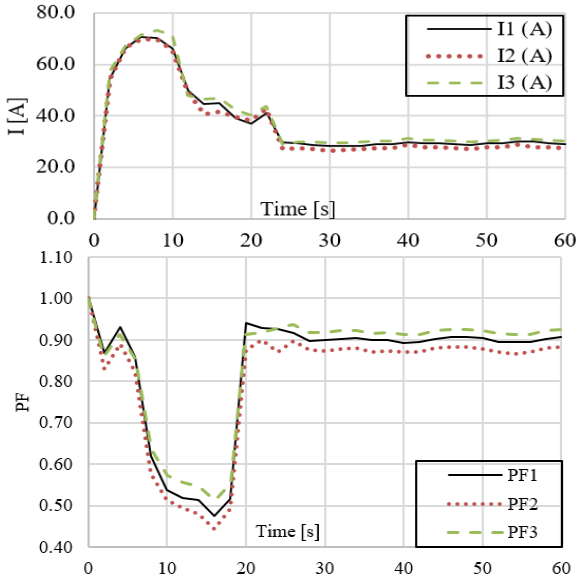

Fig. 12. Current and PF characteristics with demagnetization.

The experimental results exhibit that when the motor is partially demagnetized, the current increases, and the working current is unstable. At the same time, the PF and efficiency decreases sharply. The test results are aligned with the simulation results for the current and efficiency of the motor analyzed in the simulation section.

V. CONCLUSIONS

This study thoroughly examined the demagnetization effect during the startup of a 3000 rpm Line-Start Permanent Magnet Synchronous Motor (LSPMSM) converted from an Induction Motor (IM) featuring a 3-bar Permanent Magnet (PM) configuration. Ansys/Maxwell2D software simulations revealed that when the LSPMSM starts at high temperatures, partial PM demagnetization can occur, with the most severe impact observed in the two outermost PM pairs. Assuming these pairs experience demagnetization of 30% and 35% of their initial magnetization, the LSPMSM exhibits unstable operation at synchronous speed, intense vibrations, a 1.9-times increase in current amplitude, and a 2.7% reduction in motor efficiency compared to its non-demagnetized state.

Furthermore, the study included empirical testing using an LSPMSM prototype model. The experimental results revealed that when the LSPMSM was not demagnetized, the input phase current was approximately 26 A, exhibited a Power Factor (PF) of 0.94, and achieved a motor efficiency of 92.57%. In contrast, when the LSPMSM underwent partial demagnetization without subsequent restoration, the current increased to 28.9 A, approximately 1.1 times higher than the initial measurement. Concurrently, the PF decreased to 0.9, and the efficiency dropped to 87.19%.

The findings of this study indicate that to ensure that the LSPMSM operates with stable parameters, it is crucial to determine the appropriate PM type, method of PM arrangement, and suitable LSPMSM operating mode. This

careful selection process is necessary to prevent the irreversible partial demagnetization of the PM.

REFERENCES

[1] V. Biyani, R. Jinesh, E. T. A. Tharani, S. V. S. Sithartha, and K. P. Pinkymol, "Vector Control Implementation in PMSM Motor Drive for Electric-Vehicle Application," in *2022 4th International Conference on Energy, Power and Environment (ICEPE)*, Shillong, India, Apr. 2022, pp. 1–8, https://doi.org/10.1109/ICEPE55035.2022.9798140.

[2] N. Y. Do, T. B. Trinh, T. A. Le, and X. C. Ngo, "Rotor Configuration for Improved Working Characteristics of Lspmsm in Mining Applications," *Naukovyi Visnyk Natsionalnoho Hirnychoho Universytetu*, no. 3, pp. 79–86, 2024, https://doi.org/10.33271/nvngu/2024-3/079.

[3] A. Mahmoudi, E. Roshandel, S. Kahourzade, F. Vakilipoor, and S. Drake, "Bond Graph Model of Line-Start Permanent-Magnet Synchronous Motors," *Electrical Engineering*, vol. 106, no. 2, pp. 1667–1681, Apr. 2024, https://doi.org/10.1007/s00202-022-01654-w.

[4] N. Y. Do, T. A. Le, and X. C. Ngo, "Effect of Permanent Magnet Structure on The Performance of LSPMSM with a Power of 22 kW and 3000 rpm," *IOP Conference Series: Earth and Environmental Science*, vol. 1111, no. 1, Dec. 2022, Art. no. 012047, https://doi.org/10.1088/1755-1315/1111/1/012047.

[5] F. Yu, L. Yao, S. Chen, Y. Wang, and J.-X. Shen, "Demagnetization Analysis and Optimization Design of Interior Permanent Magnet Synchronous Motor," in *2020 23rd International Conference on Electrical Machines and Systems (ICEMS)*, Hamamatsu, Japan, Nov. 2020, pp. 704–709, https://doi.org/10.23919/ICEMS50442.2020.9291158.

[6] J. Li, J. Song, and Y. Cho, "High Performance Line Start Permanent Magnet Synchronous Motor for Pumping System," in *2010 IEEE International Symposium on Industrial Electronics*, Bari, Jul. 2010, pp. 1308–1313, https://doi.org/10.1109/ISIE.2010.5637082.

[7] P. Yu, C. Zhu, Y. Shen, and G. Zhang, "Demagnetization Analysis of Line-Start Permanent Magnet Synchronous Motors during Its Starting Process," in *2018 3rd International Conference on Electrical, Automation and Mechanical Engineering (EAME 2018)*, Jun. 2018, pp. 54–57, https://doi.org/10.2991/eame-18.2018.11.

[8] M. Baranski, W. Szelag, and W. Lyskawinski, "Analysis of the Partial Demagnetization Process of Magnets in a Line Start Permanent Magnet Synchronous Motor," *Energies*, vol. 13, no. 21, Jan. 2020, Art. no. 5562, https://doi.org/10.3390/en13215562.

[9] M. Baranski, W. Szelag, and W. Lyskawinski, "An Analysis of a Start-up Process in Lspmsms with Aluminum and Copper Rotor Bars Considering the Coupling of Electromagnetic and Thermal Phenomena," *Archives of Electrical Engineering*, vol. 68, no. 4, pp. 933–946, Dec. 2019, https://doi.org/10.24425/aee.2019.130693.

[10] A. Gozdowiak, "Coil Short-Circuit in the Stator Winding of Line-Start Permanent Magnet Synchronous Motor," *Przegląd Elektrotechniczny*, vol. 2024, no. 1, pp. 75–79, Jan. 2024, https://doi.org/10.15199/48.2024.01.15.

[11] H. Chen, X. Wang, and K. Wang, "Demagnetization Analysis of Line-Start Permanent Magnet Synchronous Motor with Composite Rotor Under Abnormal Conditions," in *2017 IEEE Transportation Electrification Conference and Expo, Asia-Pacific (ITEC Asia-Pacific)*, Harbin, China, Aug. 2017, pp. 1–6, https://doi.org/10.1109/ITEC-AP.2017.8080977.

[12] T. Zawilak, "Influence of Rotor's Cage Resistance on Demagnetization Process in the Line Start Permanent Magnet Synchronous Motor," *Archives of Electrical Engineering*, vol. 69, no. 2, pp. 249–258, 2020, https://doi.org/10.24425/aee.2020.133023.

[13] T. B. Trinh, X. C. Ngo, . A. Le, and N. Y. Do, "Effect of Permanent Magnet Structure on Working Characteristics of LSPMSM 3000 rpm," *IOP Conference Series: Earth and Environmental Science*, vol. 1275, no. 1, Nov. 2023, Art. no. 012049, https://doi.org/10.1088/1755-1315/1275/1/012049.

[14] F. Mahmouditabar, A. Vahedi, and P. Ojaghlu, "Investigation of Demagnetization Effect in an Interior V-Shaped Magnet Synchronous Motor at Dynamic and Static Conditions," *Iranian Journal of Electrical & Electronic Engineering*, vol. 14, no. 1, pp. 22-27, Mar. 2018, https://doi.org/10.22068/IJEEE.14.1.22.

[15] S. Sjökvist, "Demagnetization and Fault Simulations of Permanent Magnet Generators," PhD dissertation, Uppsala University, 2016.

[16] D. H. Bui, A. T. Le, and N. Y. Do, "A study on effect of permanent magnet configurations on starting speed curve and phase current waveform in steady state of line start magnet synchronous motors 15 kw, 3000 rpm" The University of Danang - Journal of Science and Technology, vol. 7, pp. 8-12, 2022

[17] D.-Q. Nguyen, T. N. Thai, C. L. Thi, D. B. Minh, and V. D. Quoc, "Association between the Analytical Technique and Finite Element Method for designing SPMSMs with Inner Rotor Type for Electric Vehicle Applications," *Engineering, Technology & Applied Science Research*, vol. 14, no. 3, pp. 14119–14124, Jun. 2024, https://doi.org/10.48084/etasr.7087.